

# Resistive Gas Sensor

Subjects: Chemistry, Applied

Contributor: Ze Wang

With a series of widespread applications, resistive gas sensors are considered to be promising candidates for gas detection, benefiting from their small size, ease-of-fabrication, low power consumption and outstanding maintenance properties. One-dimensional (1-D) nanomaterials, which have large specific surface areas, abundant exposed active sites and high length-to-diameter ratios, enable fast charge transfers and gas-sensitive reactions. They can also significantly enhance the sensitivity and response speed of resistive gas sensors.

Keywords: resistive gas sensor ; 1-D nanomaterial ; materials design ; gas detection ; sensing mechanism ; environment monitoring

---

## 1. Introduction

To date, many types of gas sensors with different transduction forms have been developed, e.g., catalytic combustion gas sensor <sup>[1]</sup>, electro-chemical gas sensor <sup>[2]</sup>, quartz crystal microbalance (QCM) gas sensor <sup>[3]</sup>, thermal conductivity gas sensor <sup>[4]</sup>, infrared absorption gas sensor <sup>[5]</sup> and resistive gas sensor <sup>[6][7]</sup>. Catalytic combustion gas sensors make the combustible gas burn under the effect of catalysis, and then collect the resistance value of the temperature change as the output signal <sup>[8][9]</sup>. Electro-chemical gas sensors seek to determine the gas concentration through the conversion of electrical signals after the target gas has been oxidized/reduced <sup>[10]</sup>. Thermal conductivity gas sensors can convert signals related to the type and concentration of the gas into electrical signals <sup>[4]</sup>. Infrared absorption gas sensors measure the gas concentration via the specific infrared absorption spectra of different target gases, enabling qualitative and quantitative detection simultaneously <sup>[11]</sup>. QCM gas sensors are a kind of sensitive monitoring instrument with a selective adsorption film coated on the surface of the crystal <sup>[12]</sup>. Resistive gas sensors can effectively transform the gas change around the gas-sensing medium into resistance signals, thus achieving the goal of gas sensing <sup>[13][14][15]</sup>. An ideal gas sensor must have high responsivity, good selectivity, fast response/recovery, great stability/repeatability, and low costs for practical application. Hence, six-axes spider-web diagrams for evaluating the gas-sensing properties of various sensors are shown in **Figure 1** <sup>[16][17][21][3][4][5][6][7][10]</sup>.

Compared with other gas sensors, the resistive gas sensor exhibits attractive advantages, including higher sensitivity, outstanding stability, flexibility (easy to operate and easy to utilize/integrate into portable devices), low power consumption, and lower operation cost, highlighting its great potential in gas detection, such as for environmental, safety and health monitoring <sup>[6][7][17][18][19][20][21]</sup>. However, the poor gas selectivity and high operating temperature of resistive gas sensors hinder their commercial application.

To develop high-performance resistive gas sensors, it is important to understand their gas-sensing mechanism as well as choosing suitable gas-sensing materials. The physical and chemical properties of sensing materials, such as dimension, morphology, structure, crystallinity, specific surface area, content of active sites, etc., play vital roles in the adsorption of the target gases, the electron transport and the chemical reaction rates, consequently affecting the performance of gas sensors <sup>[22][23][24][25][26]</sup>. Recently, one-dimensional (1-D) nanomaterials have become a focus for researchers. They have large surface areas, abundant exposed active sites and high length-to-diameter ratios, hence enabling fast charge transfers and efficient gas-sensitive reactions, as well as greatly enhancing the sensitivity and response speed of resistive gas sensors.

Hence, this entry firstly concentrates on the configuration type and sensing mechanism of resistive gas sensors, and further compares the characteristics of various dimensional nanomaterials applied in resistive gas sensors. Furthermore, this paper presents a comprehensive review of the recent research efforts and developments of 1-D nanomaterials as sensing materials used in resistive gas sensors, referring to the design and optimization of 1-D nanomaterials in resistive gas sensors and their potential application in the various fields of environment, safety and health monitoring ( **Figure 2** ).

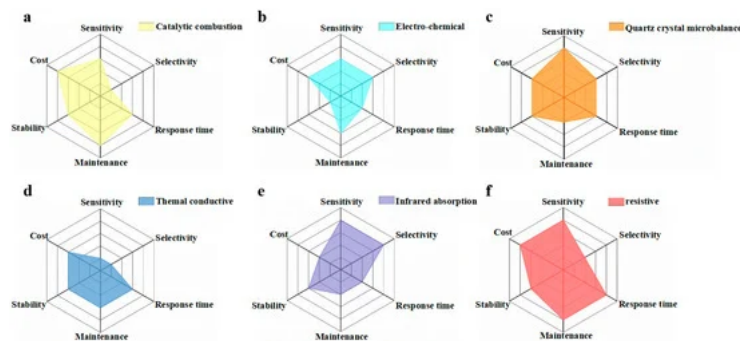


**Figure 1.** Six-axes spider-web diagrams for evaluating the gas-sensing properties of different sensors. (a) Catalytic combustion; (b) electro-chemical; (c) quartz crystal microbalance; (d) thermal conductive; (e) infrared absorption; (f) resistive gas sensors [16][17][21][31][41][51][61][71][101].

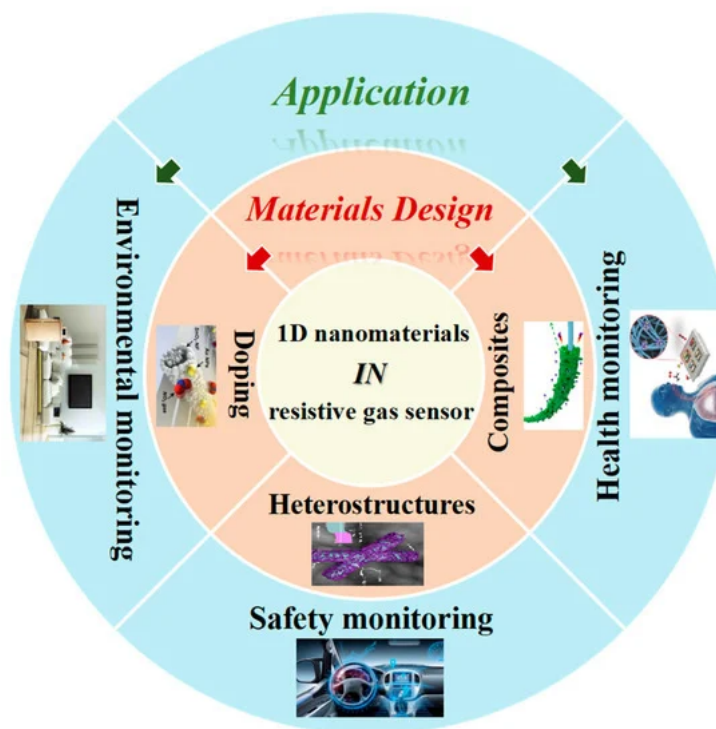


**Figure 2.** The design strategies of one-dimensional (1-D) nanomaterials and the applications of resistive gas sensors based on 1-D nanomaterials.

## 2. Introduction to Resistive Gas Sensor

To comprehensively study a resistive gas sensor, this review is carried out from four perspectives: performance index, configuration, sensing mechanism and 1-D nanomaterials.

Schematic and optical images of various resistive gas sensor configurations: (a, b) tubular [27]; (c, d) plate-like [28]; (e, f) flexible wearable [29].

The gas sensing mechanism of a metal oxide semiconductor (MOS)-based resistive sensors, for example, is predominantly based on the changes in their resistance after they are exposed to the target gases due to the chemical interaction between target gas molecules and the adsorbed oxygen ions on the surface of the MOS. There are two main sensing mechanisms, which are the surface charge layer model and the grain boundary barrier model.

Simplified gas-sensing mechanism of a space-charged model of (a) n-type and (b) p-type semiconductor metal oxides [30]; (c) schematic diagram of the proposed bifunctional sensing mechanism: reducing gas ( $H_2$ ) effect at  $SnO_2$  homointerfaces [31].

## 3. Materials Design

The main composites employed in resistive gas sensors can be divided into two categories: the conductive polymers combined with MOSs and the carbon materials combined with polymers, MOSs or metals. Building a composite system can realize synergic and complementary effects to enhance the specific physical/chemical properties of gas-sensing materials, such as electrical conductivity, mechanical strength, thermal stability, etc.

Carbon materials sense gas mainly via the detection of conductivity changes in materials caused by gas adsorption [7]. Carbon materials possess large theoretical specific surface areas, and hence can provide a large sensing area for the adsorption of gas molecules [32]. Besides, they also exhibit high carrier mobility and low resistance at room temperature [4] [33]. However, using pure carbon materials as sensing materials still has practical problems, such as poor reversibility. Therefore, various carbon-based composites have been developed and applied to gas sensors to optimize the sensing performance factors of stability, repeatability and response/recovery time.

Carbon/polymer composites have a porous microstructure, which can accelerate the adsorption and diffusion of gas molecules, promote the conductivity change rate of the sensing layer, and improve the gas sensitivity. Luo et al. [34] reported a flexible fabric gas sensor based on the rGO-PANI/cotton thread nanocomposites fabricated via the in-situ polymerization technique for the detection of sub-ppm-level NH<sub>3</sub> gas. These sensors exhibited a fast response (122 s), high sensitivity (6 to 100 ppm NH<sub>3</sub>), remarkable long-term stability (the response slightly decreased from a value of 6 after 30 days) and high selectivity (6 to NH<sub>3</sub> compared with 1.01–1.3 to others), owing to both the 1-D distinctive nanostructure and the synergistic effect between rGO nanosheets and PANI. This elaborate sensor with low power consumption is considered to be a potential flexible electronic device for the further detection of NH<sub>3</sub> gas.

The features of the current carbon gas-sensing materials used in three major compositing systems can be summarized as follows: (1) conductive polymers can improve both the selectivity and sensitivity of carbon materials, but suffer from a relatively low stability. (2) MOSs improve the sensitivity of the carbon materials to a large extent, but with long response times and poor repeatability. Metal nanoparticles can effectively catalyze the gas-sensing reaction of carbon materials; however, they exhibit poor selectivity in the mixed gas environment. Therefore, it is urgent to develop a comprehensive strategy to accelerate the practical application of carbon materials in resistive gas sensors.

## 4. Application

To date, resistive gas sensors based on 1-D nanomaterials have been widely employed in various fields, which can be mainly classified into three sections: environment, safety and health. The gases that need to be detected are obviously different in each field, thus leading to the different requirements for gas-sensitive characteristics of these 1-D gas-sensing materials, such as sensitivity, working temperature, stability, response/recovery rate, etc. Herein, resistive gas sensors based on 1-D nanomaterials for the three typical applications are further reviewed, as follows.

Traditional environmental monitoring technologies, such as mass spectrometry, gas chromatography, and optical measurement, make it possible to measure air pollutants with high precision. However, their wide application is still limited by the portability, high cost, complex operation and lack of real-time capability. In recent years, with the development of resistive gas sensors, personalized and localized environmental monitoring, rather than global and average monitoring, has received increasing attention. In the environmental field, the gases that must be monitored mainly include NO<sub>2</sub>, NH<sub>3</sub>, and some volatile organic compounds (VOCs, including formaldehyde (HCHO), methanol, toluene, etc.).

Some gases in human breath are considered to be biomarkers of disease, so it is possible to diagnose disease by detecting these characteristic gases. For example, formaldehyde (lung cancer) [35], toluene (lung cancer) [36], NH<sub>3</sub> (hemodialysis) [37], H<sub>2</sub>S (halitosis) [38], isoprene (heart disease) [39], etc. The gas sensors employed in medical diagnosis must achieve a low power consumption, and simultaneously enable the detection of trace gases at room temperature, and even be flexible and wearable in some cases.

The summary of resistive gas sensors based on 1-D nanomaterials toward different applications is shown in **Table 1**.

**Table 1.** Summary of resistive gas sensors based on 1-D nanomaterials toward different applications.

Application	Target Gas	Material	Design Strategy	Performance				
				Concentration	Response	T <sub>response</sub> /T <sub>recovery</sub> (s)	Temperature (°C)	Limit of Detection
Environmental monitoring	NO <sub>2</sub>	Au–SnO <sub>2</sub> NFs	Doping	5 ppm	180	500/223	RT	6 ppb
		WS <sub>2</sub> –SiO <sub>2</sub> NRs	Composites	5 ppm	151.2	-	RT	13.726 ppb
		ZnO NRs	-	5 ppm	70	16/200	150	1 ppm
	NH <sub>3</sub>	h-MoO <sub>3</sub> NRs	-	5 ppm	36	230/267	200	-
		CuPc–MOF-3	Heterostructures	5 ppm	45	-	RT	52 ppb
		AuGNR	Composites	25 ppm	34	224/178	RT	-
		Ag NC–MWCNTs	Composites	100 ppm	9	15/7	RT	-
	Methanol	ZnO–NiCo <sub>2</sub> O <sub>4</sub> NFs	Heterostructures	100 ppm	6.67	37/175	250	-
		Pd–CeO <sub>2</sub> NFs	Doping	100 ppm	6.95	-	200	402 ppb
		CNT–ZnO	Composites	25 ppm	72.6	3.15/3.45	250	-
	HCHO	Pt–MCN–SnO <sub>2</sub>	Doping/Heterostructures	5 ppm	33.9	-	275	50 ppb
		ZZS HNFs	Doping	100 ppm	25.7	12/45	400	500 ppb
		CdO–In <sub>2</sub> O <sub>3</sub> NTs	Heterostructures	50 ppm	72	6/12	132	100 ppb
	Toluene	Pt–TeO <sub>2</sub> –Si NW	Doping/Composites	50 ppm	45	20/500	200	-
		α-Fe <sub>2</sub> O <sub>3</sub> –NiO nanocorals	Heterostructures	50 ppm	45.4	-	350	22 ppb
Safety monitoring	H <sub>2</sub>	Au-Pt-CNFs	Doping/Composites	500 ppm	33	6.6/18	RT	-
		SnO <sub>2</sub> /NiO CSNWs	Heterostructures	500 ppm	114	120/660	500	0.9 ppm
	CO	Au–β–Ga <sub>2</sub> O <sub>3</sub> NWs	Doping	100 ppm	4.8	21.14/21.34	RT	-
		Nb–OMS–2 NFs	Doping	2 ppm	22	25/40	RT	-
		NiO–TiO <sub>2</sub> HNFs	Heterostructures	50 ppm	2.07	10/20	RT	1 ppm
		GNP–TiO <sub>2</sub> NFs	Doping	30 ppb	75	3/4	250	700 ppt
	H <sub>2</sub> S	SnO <sub>2</sub> –GO	Composites	10 ppm	17.9	12/137	70	61 ppb
		ZnO–ZnSnO <sub>3</sub> NRs	Heterostructures	30 ppm	137.9	14/26	165	700 ppb
Health monitoring	Acetone	KWO–Ti <sub>3</sub> C <sub>2</sub> T <sub>x</sub>	Composites	2.86 ppm	2.5	-	RT	-
		α-Fe <sub>2</sub> O <sub>3</sub> –SnO <sub>2</sub>	Heterostructures	1 ppm	5.37	14/70	340	0.4 ppm
		Pt–SnO <sub>2</sub> NFs	Doping	5 ppm	245.2	12.7/-	350	100 ppb
		Au–LaFeO <sub>3</sub> NBs	Doping	40 ppm	125	26/20	100	267 ppb
		PtPd–WO <sub>3</sub> NFs	Doping	1 ppm	97.5	4.2/204	300	1.07 ppb
	Ethanol	GO–PANI–PEO	Composites	200 ppm	2.1	30/252	RT	15 ppm
		Tb–In <sub>2</sub> O <sub>3</sub> NTs	Doping	100 ppm	159.8	1/60	220	-

## References

1. Del Orbe Henriquez, D.; Cho, I.; Yang, H.; Choi, J.; Kang, M.; Chang, K.S.; Jeong, C.B.; Han, S.W.; Park, I. Pt nanostructures fabricated by local hydrothermal synthesis for low-power catalytic-combustion hydrogen sensors. *ACS Appl. Nano Mater.* 2020, 4, 7–12.
2. Kim, E.B.; Seo, H.K. Highly sensitive formaldehyde detection using well-aligned Zinc oxide nanosheets synthesized by chemical bath deposition technique. *Materials* 2019, 12, 250.
3. Pérez, R.L.; Ayala, C.E.; Park, J.Y.; Choi, J.W.; Warner, I.M. Coating-based quartz crystal microbalance detection methods of environmentally relevant volatile organic compounds. *Chemosensors* 2021, 9, 153.
4. Zhang, H.Q.; Shen, B.; Hu, W.Q.; Liu, X.L. Research on a fast-response thermal conductivity sensor based on carbon nanotube modification. *Sensors* 2018, 18, 2191.
5. Chang, Y.H.; Hasan, D.; Dong, B.W.; Wei, J.X.; Ma, Y.M.; Zhou, G.Y.; Ang, K.W.; Lee, C.K. All-dielectric surface-enhanced infrared absorption-based gas sensor using guided resonance. *ACS Appl. Mater. Interfaces* 2018, 10, 38272–38279.
6. Mikołajczyk, J.; Bielecki, Z.; Stacewicz, T.; Smulko, J.; Wojtas, J.; Szabra, D.; Lentka, Ł.; Prokopiuk, A.; Magryta, P. Detection of gaseous compounds with different techniques. *Metro. Meas. Syst.* 2016, 23, 205–224.
7. Jian, Y.Y.; Hu, W.W.; Zhao, Z.H.; Cheng, P.F.; Haick, H.; Yao, M.S.; Wu, W.W. Gas sensors based on chemi-resistive hybrid functional nanomaterials. *Nano-Micro Lett.* 2020, 12, 1–43.
8. Hosoya, A.; Tamura, S.; Imanaka, N. A new catalytic combustion-type carbon monoxide gas sensor employing precious metal-free CO oxidizing catalyst. *ISIJ Int.* 2015, 55, 1699–1701.
9. Hosoya, A.; Tamura, S.; Imanaka, N. A catalytic combustion-type carbon monoxide gas sensor incorporating an apatite-type oxide. *ISIJ Int.* 2016, 56, 1634–1637.
10. Dey, A. Semiconductor metal oxide gas sensors: A review. *Mater. Sci. Eng. B* 2018, 229, 206–217.
11. Zhang, G.J.; Li, Y.P.; Li, Q.B. A miniaturized carbon dioxide gas sensor based on infrared absorption. *Opt. Lasers Eng.* 2010, 48, 1206–1212.
12. Kang, Z.J.; Zhang, D.Z.; Li, T.T.; Liu, X.H.; Song, X.S. Polydopamine-modified SnO<sub>2</sub> nanofiber composite coated QCM gas sensor for high-performance formaldehyde sensing. *Sens. Actuators B* 2021, 345, 130299.
13. Koo, W.T.; Jang, J.S.; Kim, I.D. Metal-organic frameworks for chemiresistive sensors. *Chem* 2019, 5, 1938–1963.
14. Zhao, J.J.; Losego, M.D.; Lemaire, P.C.; Williams, P.S.; Gong, B.; Atanasov, S.E.; Blevins, T.M.; Oldham, C.J.; Walls, H. J.; Shepherd, S.D.; et al. Highly adsorptive, MOF-functionalized nonwoven fiber mats for hazardous gas capture enabled by atomic layer deposition. *Adv. Mater. Interfaces* 2014, 1.
15. Chludziński, T.K.; Kwiatkowski, A. Exhaled breath analysis by resistive gas sensors. *Metro. Meas. Syst.* 2020, 27, 87–89.
16. Majhi, S.M.; Mirzaei, A.; Kim, H.W.; Kim, S.S.; Kim, T.W. Recent advances in energy-saving chemiresistive gas sensors: A review. *Nano Energy* 2021, 79, 105369.
17. Kim, J.H.; Mirzaei, A.; Kim, H.W.; Kim, S.S. Low power-consumption CO gas sensors based on Au-functionalized SnO<sub>2</sub>-ZnO core-shell nanowires. *Sens. Actuators B* 2018, 267, 597–607.
18. Huang, J.; Wan, Q. Gas sensors based on semiconducting metal oxide one-dimensional nanostructures. *Sensors* 2009, 9, 9903–9924.
19. Mirzaei, A.; Kim, J.H.; Kim, H.W.; Kim, S.S. Resistive-based gas sensors for detection of benzene, toluene and xylene (BTX) gases: A review. *J. Mater. Chem. C* 2018, 6, 4342–4370.
20. Mirzaei, A.; Lee, J.H.; Majhi, S.M.; Weber, M.; Bechelany, M.; Kim, H.W.; Kim, S.S. Resistive gas sensors based on metal-oxide nanowires. *J. Appl. Phys.* 2019, 126, 241102.
21. Wei, H.L.; Kumar, P.; Yao, D.J. Printed Resistive sensor array combined with a flexible substrate for ethanol and methane detection. *ECS J. Solid State Sci. Technol.* 2020, 9, 115008.
22. Lee, J.H. Gas sensors using hierarchical and hollow oxide nanostructures: Overview. *Sens. Actuators B* 2009, 140, 319–336.
23. Xiao, X.Y.; Zhou, X.R.; Ma, J.H.; Zhu, Y.H.; Cheng, X.W.; Luo, W.; Deng, Y.H. Rational synthesis and gas sensing performance of ordered mesoporous semiconducting WO<sub>3</sub>/NiO composites. *ACS Appl. Mater. Interfaces* 2019, 11, 26268–26276.
24. Wang, D.; Chu, X.F.; Gong, M.L. Gas-sensing properties of sensors based on single-crystalline SnO<sub>2</sub> nanorods prepared by a simple molten-salt method. *Sens. Actuators B* 2006, 117, 183–187.
25. Zhou, X.R.; Zou, Y.D.; Ma, J.D.; Cheng, X.W.; Li, Y.Y.; Deng, Y.H.; Zhao, D.Y. Cementing mesoporous ZnO with silica for controllable and switchable gas sensing selectivity. *Chem. Mater.* 2019, 31, 8112–8120.
26. Tiwari, J.N.; Tiwari, R.N.; Kim, K.S. Zero-dimensional, one-dimensional, two-dimensional and three-dimensional nanostructured materials for advanced electrochemical energy devices. *Prog. Mater. Sci.* 2012, 57, 724–803.

27. Qi, Q.; Zhang, T.; Liu, L.; Zheng, X.J. Synthesis and toluene sensing properties of SnO<sub>2</sub> nanofibers. *Sens. Actuators B* 2009, 137, 471–475.
28. Bigiani, L.; Zappa, D.; Maccato, C.; Comini, E.; Barreca, D.; Gasparotto, A. Quasi-1D MnO<sub>2</sub> nanocomposites as gas sensors for hazardous chemicals. *Appl. Surf. Sci.* 2020, 512, 145667.
29. Guo, S.Q.; Yang, D.; Zhang, S.; Dong, Q.; Li, B.C.; Tran, N.; Li, Z.Y.; Xiong, Y.J.; Zaghloul, M.E. Development of a cloud-based epidermal MoSe<sub>2</sub> Device for hazardous gas sensing. *Adv. Funct. Mater.* 2019, 29.
30. Kim, H.J.; Lee, J.H. Highly sensitive and selective gas sensors using p-type oxide semiconductors: Overview. *Sens. Actuators B* 2014, 192, 607–627.
31. Katoch, A.; Choi, S.W.; Kim, H.W.; Kim, S.S. Highly sensitive and selective H<sub>2</sub> sensing by ZnO nanofibers and the underlying sensing mechanism. *J. Hazard. Mater.* 2015, 286, 229–235.
32. Nasri, A.; Pétrissans, M.; Fierro, V.; Celzard, A. Gas sensing based on organic composite materials: Review of sensor types, progresses and challenges. *Mater. Sci. Semicond. Process.* 2021, 128.
33. Zang, X.N.; Zhou, Q.; Chang, J.Y.; Liu, Y.M.; Lin, L.W. Graphene and carbon nanotube (CNT) in MEMS/NEMS applications. *Microelectron. Eng.* 2015, 132, 192–206.
34. Luo, G.F.; Xie, L.L.; He, M.; Jaisutti, R.; Zhu, Z.G. Flexible fabric gas sensors based on reduced graphene-polyaniline nanocomposite for highly sensitive NH<sub>3</sub> detection at room temperature. *Nanotechnology* 2021, 32, 305501.
35. Güntner, A.T.; Abegg, S.; Wegner, K.; Pratsinis, S.E. Zeolite membranes for highly selective formaldehyde sensors. *Sens. Actuators B* 2018, 257, 916–923.
36. Kim, N.H.; Choi, S.J.; Yang, D.J.; Bae, J.; Park, J.; Kim, I.D. Highly sensitive and selective hydrogen sulfide and toluene sensors using Pd functionalized WO<sub>3</sub> nanofibers for potential diagnosis of halitosis and lung cancer. *Sens. Actuators B* 2014, 193, 574–581.
37. Chuang, M.Y.; Chen, C.C.; Zan, H.W.; Meng, H.F.; Lu, C.J. Organic gas sensor with an improved lifetime for detecting breath ammonia in hemodialysis patients. *ACS Sens.* 2017, 2, 1788–1795.
38. Lee, I.; Choi, S.J.; Park, K.M.; Lee, S.S.; Choi, S.; Kim, I.D.; Park, C.O. The stability, sensitivity and response transients of ZnO, SnO<sub>2</sub> and WO<sub>3</sub> sensors under acetone, toluene and H<sub>2</sub>S environments. *Sens. Actuators B* 2014, 197, 300–307.
39. Van den Broek, J.; Guntner, A.T.; Pratsinis, S.E. Highly selective and rapid breath isoprene sensing enabled by activated alumina filter. *ACS Sens.* 2018, 3, 677–683.
40. Lim, K.; Jo, Y.M.; Yoon, J.W.; Kim, J.S.; Lee, D.J.; Moon, Y.K.; Yoon, J.W.; Kim, J.H.; Choi, H.J.; Lee, J.H. A transparent nanopatterned chemiresistor: Visible-light plasmonic sensor for trace-level NO<sub>2</sub> detection at room temperature. *Small* 2021, e2100438.
41. Suh, J.M.; Kwon, K.C.; Lee, T.H.; Kim, C.; Lee, C.W.; Song, Y.G.; Choi, M.J.; Choi, S.; Cho, S.H.; Kim, S.; et al. Edge-exposed WS<sub>2</sub> on 1D nanostructures for highly selective NO<sub>2</sub> sensor at room temperature. *Sens. Actuators B* 2021, 333, 129566.
42. Godse, P.R.; Mane, A.T.; Navale, Y.H.; Navale, S.T.; Mulik, R.N.; Patil, V.B. Hydrothermally grown 1D ZnO nanostructures for rapid detection of NO<sub>2</sub> gas. *SN Appl. Sci.* 2021, 3.
43. Kumar, S.; Singh, A.; Singh, R.; Singh, S.; Kumar, P.; Kumar, R. Facile h-MoO<sub>3</sub> synthesis for NH<sub>3</sub> gas sensing application at moderate operating temperature. *Sens. Actuators B* 2020, 325, 128974.
44. Zheng, J.Z.; Pang, K.L.; Liu, X.; Li, S.X.; Song, R.; Liu, Y.L.; Tang, Z.Y. Integration and synergy of organic single crystals and metal-organic frameworks in core-shell heterostructures enables outstanding gas selectivity for detection. *Adv. Funct. Mater.* 2020, 30.
45. Seifaddini, P.; Ghasempour, R.; Ramezannezhad, M.; Nikfarjam, A. Room temperature ammonia gas sensor based on Au/graphene nanoribbon. *Mater. Res. Express* 2019, 6, 045054.
46. Cui, S.M.; Pu, H.H.; Lu, G.H.; Wen, Z.H.; Mattson, E.C.; Hirschmugl, C.; Gajdardziska-Josifovska, M.; Weinert, M.; Chen, J.H. Fast and selective room-temperature ammonia sensors using silver nanocrystal-functionalized carbon nanotubes. *ACS Appl. Mater. Interfaces* 2012, 4, 4898–4904.
47. Liang, Y.; Liu, W.H.; Hu, W.; Zhou, Q.H.; He, K.R.; Xu, K.; Yang, Y.; Yu, T.; Yuan, C.L. Synthesis and gas-sensing properties of [email protected]2O<sub>4</sub> [email protected] nanofibers. *Mater. Res. Bull.* 2019, 114, 1–9.
48. Hu, Q.; Huang, B.Y.; Li, Y.; Zhang, S.M.; Zhang, Y.X.; Hua, X.H.; Liu, G.; Li, B.S.; Zhou, J.Y.; Xie, E.Q.; et al. Methanol gas detection of electrospun CeO<sub>2</sub> nanofibers by regulating Ce<sup>3+</sup>/Ce<sup>4+</sup> mole ratio via Pd doping. *Sens. Actuators B* 2020, 307, 127638.
49. Sinha, M.; Neogi, S.; Mahapatra, R.; Krishnamurthy, S.; Ghosh, R. Material dependent and temperature driven adsorption on switching (p- to n- type) using CNT/ZnO composite-based chemiresistive methanol gas sensor. *Sens. Actuators B* 2021, 336, 129729.
50. Shin, H.; Jung, W.G.; Kim, D.H.; Jang, J.S.; Kim, Y.H.; Koo, W.T.; Bae, J.; Park, C.; Cho, S.H.; Kim, B.J.; et al. Single-atom Pt stabilized on one-dimensional nanostructure support via carbon nitride/SnO<sub>2</sub> heterojunction trapping. *ACS Nano* 2020, 14, 11394–11405.

51. Zhu, L.; Wang, J.N.; Liu, J.W.; Nasir, M.S.; Zhu, J.W.; Li, S.S.; Liang, J.D.; Yan, W. Smart formaldehyde detection enabled by metal organic framework-derived doped electrospun hollow nanofibers. *Sens. Actuators B* 2021, 326, 128819.
52. Zeng, X.G.; Wang, Z.; Li, Y.; Li, H.Y.; Xu, S.Y.; Liu, L.; Gong, Y.M.; Liang, Q.C.; Duan, H.J.; Cheng, Y.L.; et al. Highly sensitive and selective formaldehyde gas sensor based on CdO–In<sub>2</sub>O<sub>3</sub> beaded porous nanotubes at low temperature. *J. Mater. Sci. Mater. Electron.* 2018, 29, 17533–17541.
53. Bang, J.H.; Choi, M.S.; Mirzaei, A.; Han, S.; Lee, H.Y.; Choi, S.W.; Kim, S.S.; Kim, H.W. Hybridization of silicon nanowires with TeO<sub>2</sub> branch structures and Pt nanoparticles for highly sensitive and selective toluene sensing. *Appl. Surf. Sci.* 2020, 525, 146620.
54. Suh, J.M.; Shim, Y.S.; Kim, D.H.; Sohn, W.; Jung, Y.M.; Lee, S.Y.; Choi, S.; Kim, Y.H.; Jeon, J.M.; Hong, K.; et al. Synergistically selective toluene sensing in hematite-decorated nickel oxide nanocorals. *Adv. Mater. Technol.* 2017, 2.
55. Nair, K.G.; Ramakrishnan, V.; Unnathpadi, R.; Karuppanan, K.K.; Pullithadathil, B. Unraveling hydrogen adsorption kinetics of bimetallic Au–Pt nanoisland-functionalized carbon nanofibers for room-temperature Gas sensor applications. *J. Phys. Chem. C* 2020, 124, 7144–7155.
56. Raza, M.H.; Kaur, N.; Comini, E.; Pinna, N. Toward optimized radial modulation of the space-charge region in one-dimensional SnO<sub>2</sub>–NiO core-shell nanowires for hydrogen sensing. *ACS Appl. Mater. Interfaces* 2020, 12, 4594–4606.
57. Weng, T.F.; Ho, M.S.; Sivakumar, C.; Balraj, B.; Chung, P.F. VLS growth of pure and Au decorated  $\beta$ -Ga<sub>2</sub>O<sub>3</sub> nanowires for room temperature CO gas sensor and resistive memory applications. *Appl. Surf. Sci.* 2020, 533, 147476.
58. Kumar, R.; Jaiswal, M.; Singh, O.; Gupta, A.; Ansari, M.S.; Mittal, J. Selective and reversible sensing of low concentration of carbon monoxide gas using Nb-doped OMS-2 nanofibers at room temperature. *IEEE Sens. J.* 2019, 19, 7201–7206.
59. Wang, L.L.; Chai, R.Q.; Lou, Z.; Shen, G.Z. Highly sensitive hybrid nanofiber-based room-temperature CO sensors: Experiments and density functional theory simulations. *Nano Res.* 2017, 11, 1029–1037.
60. Nikfarjam, A.; Hosseini, S.; Salehifar, N. Fabrication of a highly sensitive single aligned TiO<sub>2</sub> and gold nanoparticle embedded TiO<sub>2</sub> nano-fiber Gas sensor. *ACS Appl. Mater. Interfaces* 2017, 9, 15662–15671.
61. Gu, H.H.; Wang, Z.; Hu, Y.M. Hydrogen gas sensors based on semiconductor oxide nanostructures. *Sensors* 2012, 12, 5517–5550.
62. Wang, Y.; Gao, P.; Sha, L.N.; Chi, Q.Q.; Yang, L.; Zhang, J.J.; Chen, Y.J.; Zhang, M.L. Spatial separation of electrons and holes for enhancing the gas-sensing property of a semiconductor: ZnO/ZnSnO<sub>3</sub> nanorod arrays prepared by a hetero-epitaxial growth. *Nanotechnology* 2018, 29, 175501.
63. Ama, O.; Sadiq, M.; Johnson, M.; Zhang, Q.F.; Wang, D.L. Novel 1D/2D KWO/Ti<sub>3</sub>C<sub>2</sub>Tx nanocomposite-based acetone sensor for diabetes prevention and monitoring. *Chemosensors* 2020, 8, 102.
64. Gong, H.M.; Zhao, C.H.; Niu, G.Q.; Zhang, W.; Wang, F. Construction of 1D/2D  $\alpha$ -Fe<sub>2</sub>O<sub>3</sub>/SnO<sub>2</sub> hybrid nanoarrays for or sub-ppm acetone detection. *Research (Wash D C)* 2020, 2020, 2196063.
65. Kim, D.H.; Jang, J.S.; Koo, W.T.; Kim, I.D. Graphene oxide templating: Facile synthesis of morphology engineered crumpled SnO<sub>2</sub> nanofibers for superior chemiresistors. *J. Mater. Chem. A* 2018, 6, 13825–13834.
66. Shingange, K.; Swart, H.; Mhlongo, G.H. Ultrafast detection of low acetone concentration displayed by Au-loaded LaFeO<sub>3</sub> nanobelts owing to synergetic effects of porous 1D morphology and catalytic activity of Au nanoparticles. *ACS Omega* 2019, 4, 19018–19029.
67. Kim, S.J.; Choi, S.J.; Jang, J.S.; Cho, H.J.; Koo, W.T.; Tuller, H.L.; Kim, I.D. Exceptional high-performance of Pt-based bimetallic catalysts for exclusive detection of exhaled biomarkers. *Adv. Mater.* 2017, 29.
68. Burris, A.J.; Tran, K.; Cheng, Q. Tunable enhancement of a graphene/polyaniline/poly(ethylene oxide) composite electrospun nanofiber gas sensor. *J. Anal. Test.* 2017, 1, 12.
69. Bai, J.L.; Luo, Y.B.; Chen, C.; Deng, Y.; Cheng, X.; An, B.X.; Wang, Q.; Li, J.P.; Zhou, J.Y.; Wang, Y.R.; et al. Functionalization of 1D In<sub>2</sub>O<sub>3</sub> nanotubes with abundant oxygen vacancies by rare earth dopant for ultra-high sensitive ethanol detection. *Sens. Actuators B* 2020, 324, 128755.